

# TWO DECADES OF MULTI-SENSOR SUBSIDENCE MONITORING OVER EBRO DELTA USING COHERENCE-BASED DINSAR TECHNIQUES

Pipia Luca<sup>(1)</sup>, Pérez Fernando<sup>(1)</sup>, Marturià Jordi<sup>(1)</sup>, Corbera Jordi<sup>(1)</sup>, Jornet Lluís<sup>(2)</sup>, Rovira Albert<sup>(2)</sup>

<sup>(1)</sup> Institut Cartogràfic i Geològic de Catalunya (ICGC), Barcelona, Spain

Email: {luca.pipia, fernando.perez, jordi.marturia, jordi.corbera}@icgc.cat

<sup>(2)</sup> Aquatic Ecosystems - Institut Recerca i Tecnologia Agroalimentària (IRTA), Sant Carles de la Ràpita, Spain

Email: {lluis.jornet, albert.rovira}@irta.cat

## ABSTRACT

This work presents the historical study of the subsidence phenomenon over the Ebro Delta plain carried out as WPB6 in the frame of Ebro-ADMICLIM LIFE project, using coherence-based differential interferometric SAR techniques (DInSAR). To this end, the whole SAR archive available at ESA over the area of interest (AOI) at C-Band and L-Band has been analyzed. The results provided by each stack term of absolute deformation and deformation-rate maps are first shown. Then, a space-time filtering method to take advantage of the redundant information provided by ERS and ENVISAT data is put forward. C-band and L-band retrievals are then compared, and future monitoring activity based on Sentinel-1 imaging is discussed.

## 1. INTRODUCTION

The Ebro River Delta represents a vulnerable area in South Catalonia (Spain) due to both rising sea level and subsidence phenomena. Usually, deltaic areas are characterized by natural compaction of sediment layers accumulated during geological eras, with consequent modification of ground elevation. The rate of accumulation-compaction is a key factor, along with coastal dynamics and sea level change, to be monitored in order to preserve such an area: an increase or decrease of the extension of the surface area of Delta plain induces changes in the chemical properties of soil and aquifer dynamics. Ebro-ADMICLIM (LIFE13 ENV/ES/001182 - B1) is a European co-funded project focused on the adaptation and mitigation measures in Ebro Delta to face climate change. The project's main goal is to work out an integrated approach to deal with water management, sediment and habitat dynamics, coastal erosion, carbon sequestration in the soil, greenhouse gases (GHG) emissions and water quality improvement. In other words, the idea is to jointly manage the contributions of inorganic (sediments) and organic matter to the soil, with the aim to optimize the processes of vertical accretion (soil formation) and decomposition of organic matter (GHG emission) in the rice fields and constructed wetlands. It is worth mentioning that this is a breakthrough approach, which has been never applied so far in the European Union.



Figure 1: Detail of the Area of Interest, corresponding to the Ebro River Delta.

## 2. AREA OF INTEREST AND DATASET

The Area of Interest (AOI), shown in Figure 1, is particularly tricky for long-term SAR studies, due to the low-coherence values characterizing the Ebro plain land covers, mainly rice fields, wetlands and mudflats. As a consequence, coherent areas can only be found over a few urbanized areas, corresponding to small villages, and isolated farms unevenly scattered over Delta.

The available datasets spanned over an observation period of approximately 20 years, and were made up of 8 differential stacks: 1 ascending and 3 descending stacks for ERS1 and ERS2 plus 2 ascending and 2 descending stacks for ENVISAT. Besides, a stack of 12 ALOS-PALSAR images covering the period 2007-2011 was also made available by JAXA as ESA Third-Party Mission Data. Details about the data collected are reported in Table 1.

SENSOR	ORBIT	Type	# Images	Start Date	Final Date	Band
ERS1	287	ASC	15	04-06-95	28-05-00	C
ERS1	194	DESC	11	19-06-92	07-04-96	C
ERS2	194	DESC	32	07-08-95	13-11-00	C
ERS2	283	DESC	32	19-06-95	29-11-00	C
ENVISAT	015	ASC	27	14-01-03	10-08-10	C
ENVISAT	287	ASC	25	09-03-03	18-10-09	C
ENVISAT	194	DESC	26	25-10-03	23-10-10	C
ENVISAT	423	DESC	27	08-01-03	04-08-10	C
PALSAR	194	ASC	12	12-07-07	08-03-11	L

Table 1: Differential interferometric datasets available over the AOI in the ESA Catalogue.

## 3. C-BAND PROCESSING

For the processing of C-Band stacks, the Grid Processing on Demand (G-POD) service of the European Space Agency (ESA), based on the Small-

Baseline (SBAS) technique developed by IREA-CNR [1] has been employed. In order to guarantee the meaningfulness of result comparisons in terms of deformation-rate and absolute deformation, the same seed location and the same SBAS configuration parameters have been used.

G-POD SBAS SERVICE SETTING PARAMETERS	
Seed Coordinates (UTM-ETRS89)	303762E, 4519312N
Max Perpendicular Baseline	400 m
Max Temporal Baseline	1000 days
Maxi Allowed Doppler Centroid	1000 Hz, 2000 Hz
Multilook Factor	6 (rg) x 20 (az)
Ground Pixel Dimension	80 m
Goldstein Weight	0.5
Coherence Threshold	0.5
APS Smoothing Time Window	200 days

Table 2: G-POD SBAS Setting Parameters

The images reported in Figure 2 show the result provided by G-POD SBAS in terms of absolute deformation and deformation rate information over the AOI concerning 6 of the 8 available datasets. It can be observed the lack of coherent areas over most of the Deltaic area, due to the long observation period as well as the short temporal correlation of rice fields, wetlands and mudflats.

Yet, the availability of multiple stacks relative to the same observation period offers the possibility to improve the estimation of the subsidence phenomenon over the AOI using digital filtering techniques.

#### 4. C-BAND DATA HOMOGENIZAYION

In order to improve the deformation rate map over the AOI using the redundant information made available by the multiple DInSAR stacks, a specific space-time filtering strategy has been developed. It is made up by three main steps sketched in Figure 3:

1. Spatial Search
2. Time Averaging
3. Long-Term Synthesis

For the entire area of interest a synthetic UTM grid is defined. For each point P of the grid, the absolute deformations of all the pixels from each C-band stack at a radial distance from P lower than a maximum threshold are stored. Next, a synthetic time vector covering the whole observation period and the absolute deformation of pixels selected at step 1 are averaged using a fixed time window around each date in this vector. For each point of the spatial mesh, two time-averaged deformation profiles are generated: one for the ERS collections and another one for ENVISAT observations, since they do not overlap in the timeline. Finally, the time-averaged ENVISAT deformation profile is offset-corrected taking into account the linear trend of the ERS-based information. The offset is calculated as the difference between both linear trends at the time corresponding to the first date of ENVISAT synthetic profile.

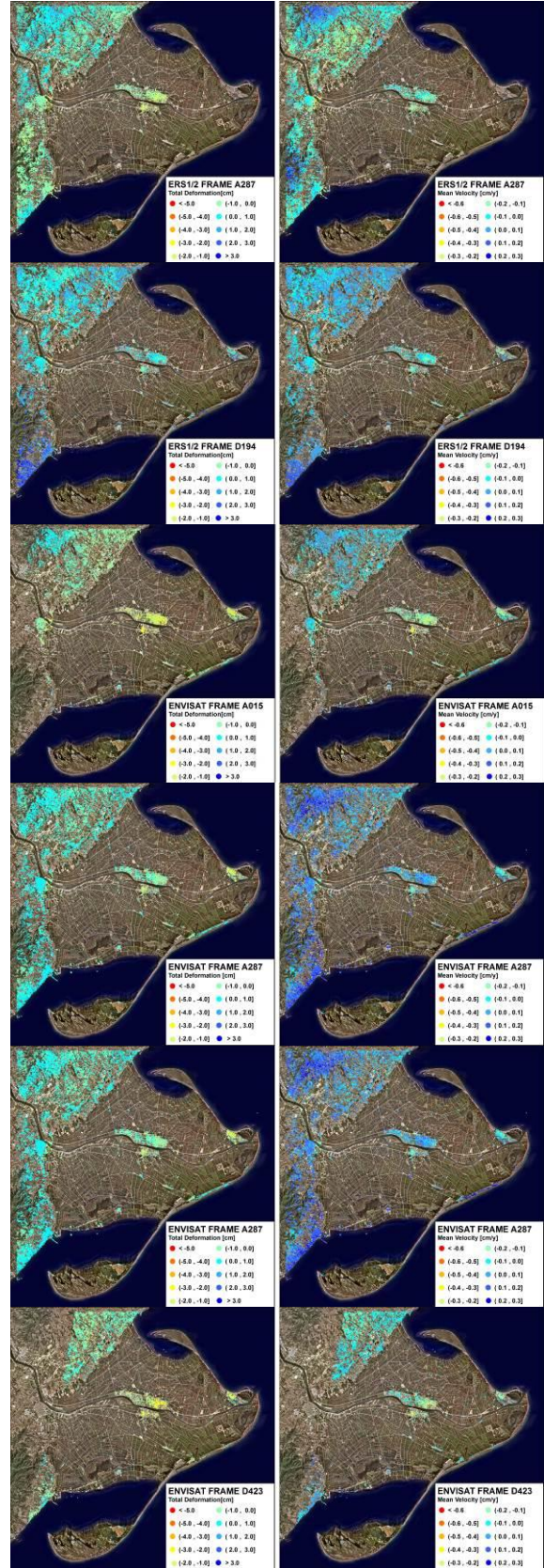


Figure 2: Example of AOI absolute deformation and deformation-rate maps retrieved at C-band from ERS and ENVISAT imaging.

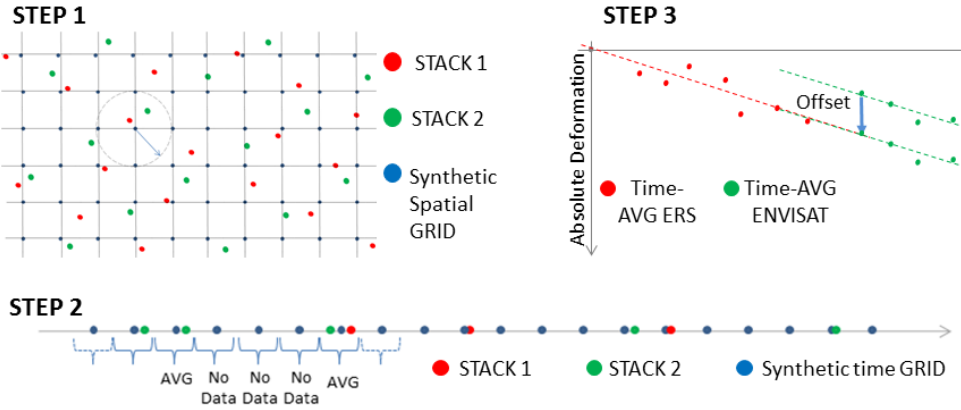


Figure 3: Sketches of the 3 main steps of the space-time filtering strategy

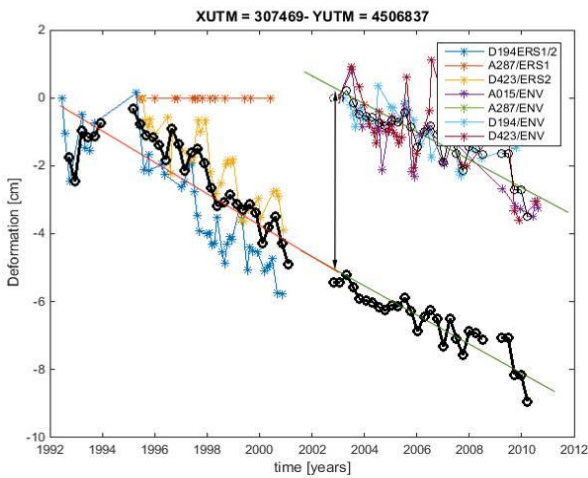


Figure 4: Space-time filtering strategy applied to real data.

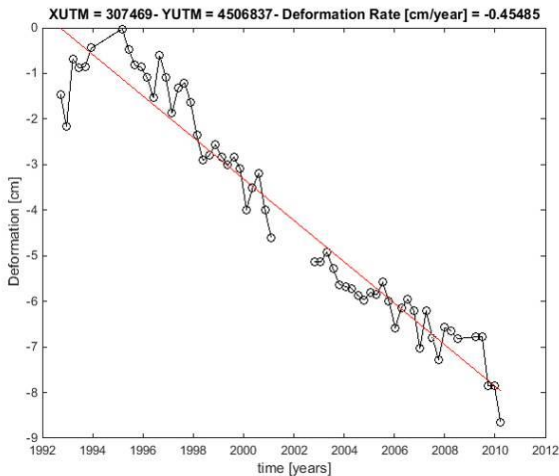


Figure 5: Long-term deformation rate estimation over the space-time averaged absolute deformation profile.

The profiles in Figure 4 show an example of the time-filtering procedure applied to the whole collection of C-band stacks for a point ( $X_{UTM}, Y_{UTM}$ ) of the synthetic grid. In this case, the first available information comes from ERS1-194 stack, the only one starting in 1992.

The Absolute Deformation Profile (ADP) of any other ERS1 stack is vertically shifted to the deformation value of ERS1-194 profile at the time closest to the first acquisition of each of the new stacks. Afterwards, ERS1 time-averaged ADP (TAADP) is calculated along a synthetic time vector and line-fitted (red straight line). The same procedure is then applied to ENVISAT deformation profiles, and the obtained TAADP is line-fitted (green straight line). Finally, ENVISAT TAADP is offset-corrected as follows: the new value of green line at the first meaningful date of ENVISAT TAADP corresponds to the value of ERS-based regression line at that date. The last step of the filtering strategy carries out the estimation of the long-term deformation rate by linearly fitting the ERS-ENVISAT time averaged profile at pixel level.

For points in the synthetic grid with no pixels from ERS1-194 stack falling within the searching radius, the first offset estimation is simply skipped. The possible different time-zero for the interpolation process is not an issue, since the aim of the time-average operation is only the estimation of the trend (rate) of the subsidence phenomena, whose linearity is demonstrated by the absolute deformation profiles provided by each stack separately. In this evidence, it is meaningful to generate a synthetic cumulative deformation map covering the whole observation period (1992-2010). The result obtained in terms of long-term deformation rate map and long-term total deformation is shown in Figure 6 and Figure 7, respectively.

## 5. L-BAND PROCESSING

For the processing of ALOS-PALSAR stack, the ICGC Advanced DInSAR Processing Chain based on Coherent Pixel Technique was employed [3]. The deformation rate map retrieved at L-band is depicted in Figure 7.

Note the presence of coherent pixels distributed along regular patterns all over the Ebro Delta area. They correspond to ditches used for rice field irrigation.

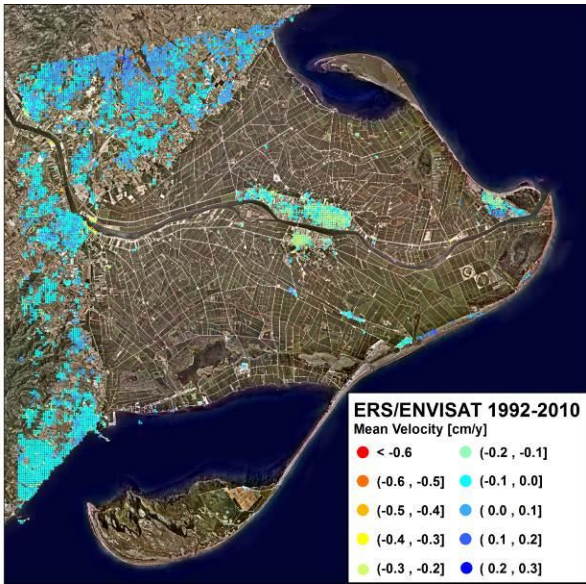


Figure 6: Deformation rate map over the AOI provided by the space-time filtering strategy.

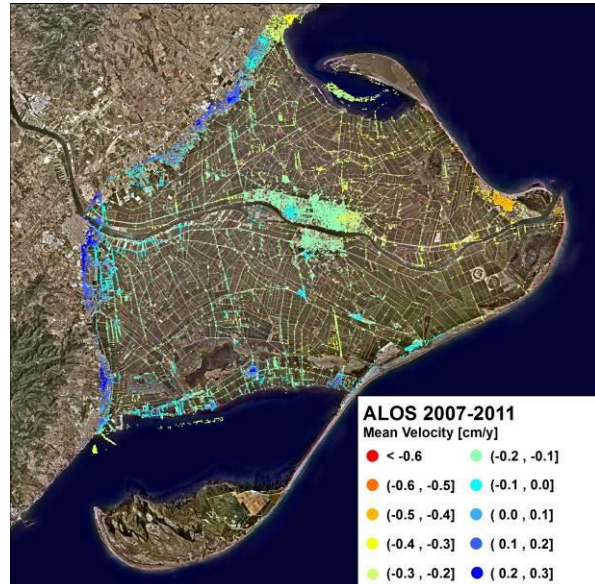


Figure 7: Deformation rate map retrieved at L-Band using ALOS imaging.

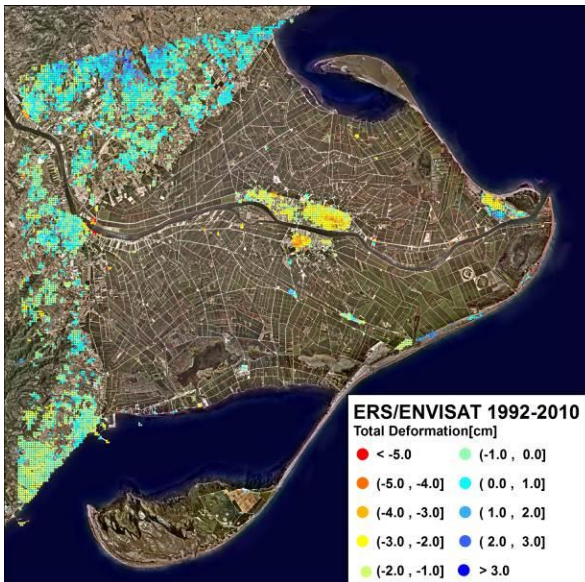


Figure 8: Total deformation map (1992-2010) over the AOI provided by the space-time filtering strategy.

Being the illumination angle quite close among the 3 satellites, the more stable response here observed could be ascribed to the longer wavelength, better spatial resolution and/or shorter time span.

The higher deformation rate over specific areas (i.e. Riumar, in the Northern part of Delta tip) might be induced by hydrological fluctuations or anthropic water use. These changes are smoothed by the longer observation window of C-Band analysis.

In order to compare L- and C-Band retrievals on the overlapping time span, the L-Band absolute deformation profile must be properly tied to the long-time synthetic profile. The criterion followed in this work applies an

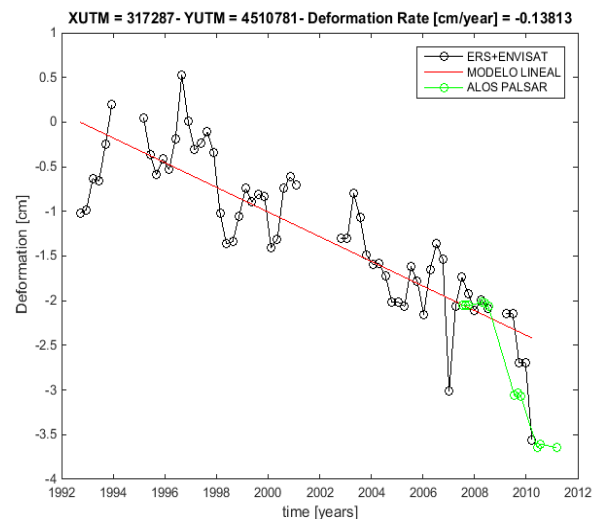


Figure 9: L-Band ALOS absolute deformation (green) tied to C-band space-time filtered absolute deformation.

offset to the deformation value at the time of the first ALOS image (theoretically zero, being the starting point of the time series) corresponding to the value provided by the long-term deformation rate at the same date.

In Figure 9, it is shown in black the long-term absolute deformation profile of a pixel selected within the urban area of Riumar, and in green the absolute deformation provided by ALOS study, properly tied to the linear trend of C-band estimation.

A good matching between both estimates can be observed in terms of total amount of absolute deformation over the overlapping observation period, between 2007 and 2010.

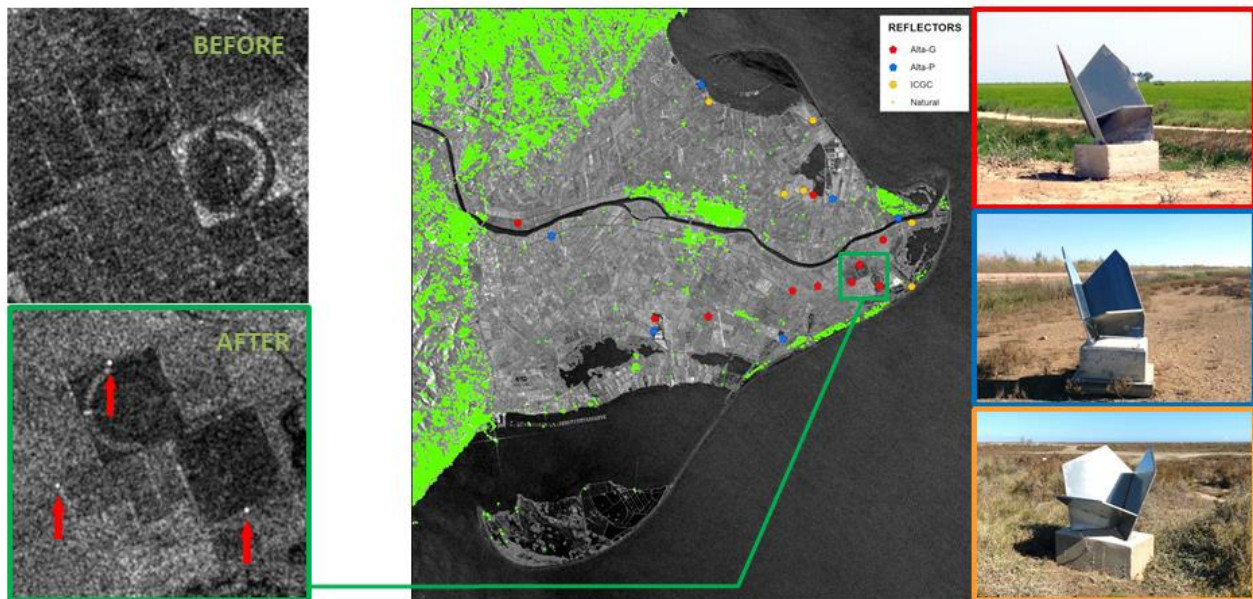


Figure 10: Distribution of the three types of corner reflectors (right images) over a S1 image of the AOI (centre), and an example of their response by comparison of SAR backscattering before and after CRs installation (left images).

## 6. ONGOING MONITORING

The project continues with the monitoring of the area through Sentinel-1 SAR images combining 2 frames (one ascending, one descending) routinely acquired over the AOI. In order to compensate for the few coherent areas over the Ebro Delta plain and the relatively low spatial resolution of S-1 images, 22 corner reflectors (CRs) have been deployed in the AOI in the framework of the Ebro-ADMICLIM Life project. The aim is to take advantage of the shorter revisit time of S-1 and preserve the spatial resolution, moving from a coherent- to an amplitude-based approach. The images in **Figure 10** present an S-1 image showing the strategical distribution of three types of CRs over the AOI together with the coherent points provided by the C-band analysis, as well as an example of the SAR response before and after the installation of a CR. Being a *harsh* environment for CRs, its visibility is routinely monitored.

## 7. CONCLUSIONS

The work here presented demonstrates the existence of very slow subsidence phenomena (~3mm/year) that has been affecting the Ebro Delta plain during the last 2 decades. Deformation fluctuations could be induced by hydrological processes, also explaining the higher deformation rate estimated at L-Band in the shorter observation period.

Further studies based on S1 acquisitions will help to assess the stability of this trend, taking also advantage of the stable response of the CRs deployed in the AOI.

## 8. ACKNOWLEDGMENTS

The authors would like to thank ESA for providing the SAR data used in this work (ESA Project ID 28768) and CNR-IREA staff for the help in processing C-Band stacks using G-POD SBAS InSAR service.

## 9. REFERENCES

1. F. Casu, S. Elefante, P. Imperatore, I. Zinno, M. Manunta, C. De Luca, R. Lanari, "SBAS-DInSAR Parallel Processing for Deformation Time-Series Computation," *IEEE JSTARS*, vol. 7, no. 8, pp. 3285-3296, 2014, Doi: 10.1109/JSTARS.2014.2322671
2. Blanco Sánchez P., Mallorqui J., Duque S., Modells D., "The Coherent Pixels Technique (CPT): An Advanced DInSAR Technique for Nonlinear Deformation Monitoring" *Pure & applied geophysics PAGEOPH*, Vol. 165, No. 6, pp. 1167-1193.
3. Ferretti A., Prati C., Rocca F., "Permanent Scatterers in SAR interferometry," *IEEE Transactions on Geoscience and Remote Sensing*, Vol 39, No. 1,